Hindawi Publishing Corporation
Advances in Chemistry
Volume 2016, Article ID 7297268, 9 pages
http://dx.doi.org/10.1155/2016/7297268

Research Article

A Computational and Experimental Study of the Conformers of Pyrrolidinium Ionic Liquid Cations Containing an Ethoxy Group in the Alkyl Side Chain

Francesco Trequattrini,[1,2] Oriele Palumbo,[1] Sara Gatto,[1] Giovanni Battista Appetecchi,[3] and Annalisa Paolone[1]

[1]*CNR-ISC, U.O.S. La Sapienza, Piazzale A. Moro 5, 00185 Roma, Italy*
[2]*Physics Department, Sapienza University of Rome, Piazzale A. Moro 5, 00185 Rome, Italy*
[3]*ENEA, Materials and Physicochemical Processes Laboratory (SSPT-PROMAS-MATPRO), Via Anguillarese 301, 00123 Rome, Italy*

Correspondence should be addressed to Annalisa Paolone; annalisa.paolone@roma1.infn.it

Received 27 April 2016; Accepted 10 July 2016

Academic Editor: Dheeraj K. Singh

We investigate the conformers of the *N*-methoxyethyl-*N*-methylpyrrolidinium ($PYR_{1(2O1)}$) and *N*-ethoxyethyl-*N*-methylpyrrolidinium ($PYR_{1(2O2)}$) ionic liquid cations by means of DFT calculations at the B3LYP/6-31G** level and we calculate their infrared vibration frequencies. The comparison with the absorbance spectra of two ionic liquids containing these ions indicates good performance of such a combination of theory and basis set. The lowest energy conformer of each pyrrolidinium cation displays equatorial-envelope geometry; however, in contrast with the prototypical PYR_{14}, the main alkyl side chain is not in an all-*trans* configuration, but it tends to be bent. Moreover, calculations indicate that the LUMO orbital extends more along the alkyl side chain in $PYR_{1(2O1)}$ and $PYR_{1(2O2)}$ than in the parent ion 1-butyl-1-methylpyrrolidinium (PYR_{14}).

1. Introduction

Ionic liquids are salts with melting points lower than 100°C. The large variety of possible anions and cations allows tailoring their physiochemical properties, such as viscosity, electrical conductivity, melting point, or glass transition temperature. They are considered as promising safe electrolyte components for lithium batteries and, more broadly, for a wide variety of electrochemical devices, especially the family with pyrrolidinium cations and per(fluoroalkylsulfonyl)imide anions, due to the subambient melting temperature, high room temperature conductivity, and suitable electrochemical stability [1]. One of the most studied ILs is 1-butyl-1-methylpyrrolidinium bis(trifluoromethanesulfonyl)imide (PYR_{14}TFSI). It displays a rich phase diagram as a function of temperature [2]: on cooling it undergoes a glass transition around −85°C; on subsequent heating, it is devitrified and enters an undercooled region; at ~−63°C it crystallizes and around −30°C it undergoes a solid-solid phase transition; finally it melts at ~−7°C. PYR_{14}TFSI has been largely investigated by means of vibrational spectroscopy, aided by DFT calculations [3–8]. Both the TFSI anion and PYR_{14} cation possess conformers, due to the flexibility of the chemical bonds. TFSI has two conformers: the *transoid* one with C_2 symmetry is more stable than the *cisoid* one which has C_1 symmetry [8–10]. However, the two conformers are energetically separated by only 2.2 kJ mol^{-1}. The *cisoid* and *transoid* forms of TFSI give different Raman and infrared spectra, as confirmed by experimental and computational studies [8, 11–13]. In particular, the infrared spectral lines observed at ~600 and 650 cm^{-1} can be assigned to the *cis* conformer, whereas the line at ~620 cm^{-1} can be assigned to *trans*-TFSI [5–8].

Concerning the PYR_{14} cation, some detailed studies linking the geometry of the ion with the vibrational properties are available [3, 4, 14, 15]. In these studies, the Raman spectra and

the computed Raman activities are reported [3, 4, 14, 15]. DFT calculations evidenced that the occurrence of conformers of the pyrrolidinium ion is due to the fact that the C_4N ring is not planar and can therefore adopt either the *envelope* or the *twist* configuration [3, 4, 14–16]. In the first case, one of the atoms is located outside the plane defined by the other four atoms; on the contrary, in the *twist* configuration, two atoms are located above and below the plane constructed by the other three atoms. The *envelope* and *twist* conformers can easily convert one into the other by means of pseudorotations, as the difference in energy between the different conformers can be as low as ~2.6 kJ mol^{-1} [14, 15]. It has been reported [14, 16] that, among others, the equatorial-envelope and axial-envelope conformers with the butyl group at equatorial and axial positions against the four carbon atoms of the pyrrolidinium ring are relatively stable, and the equatorial-envelope conformer gives the global minimum. The same authors suggested that these two conformers are present in equilibrium in molten PYR_{14}TFSI [14].

Previous systematic studies of the conformers of the ions composing ILs have been reported for TFSI and PYR_{14} [3, 4, 12–14], bis(fluorosulfonyl)imide (FSI) [15–17], N,N-diethyl-N-methyl-N-propylammonium [18], imidazolium [11, 19–22], and ammonium ions [23, 24]. It must be noted that the presence of different conformers can alter the physicochemical properties of ILs. For example, it has been reported that ionic liquids containing different conformers have different melting points [25]. It is, therefore, important to investigate the possible occurrence of various conformers of new ions. In this context, a combination of DFT calculations and vibrational spectroscopies, such as Raman or infrared, are extremely useful.

Recently, looking for better performances of ionic liquids of the pyrrolidinium family, some modifications of the alkyl chain have been proposed with the aim of decreasing the temperature at which solid phases are formed and having greater flexibility of the chain. Indeed, when an oxygen atom is introduced in the alkyl chain of the pyrrolidinium ion, no crystallization was detected down to −150°C for $PYR_{1(2O1)}$TFSI and $PYR_{1(2O1)}IM_{14}$ [26–30].

To the best of our knowledge, the conformers of pyrrolidinium cations containing an ethoxy group in the main aliphatic side chain and their vibrational spectra have never been studied. The aim of the present work is to fill this gap, by means of a combination of DFT calculations and experimental investigations of the infrared spectra of two ILs as a function of temperature: $PYR_{1(2O1)}$TFSI and $PYR_{1(2O1)}$FSI. For comparison, also the conformers of PYR_{14} will be investigated again by means of DFT calculations.

2. Materials and Methods

2.1. Experimental. *N*-methoxyethyl-*N*-methylpyrrolidinium bis(trifluoromethanesulfonyl)imide ($PYR_{1(2O1)}$TFSI) and *N*-ethoxyethyl-*N*-methylpyrrolidinium bis(fluorosulfonyl)imide ($PYR_{1(2O2)}$FSI) were synthesized as reported in [26, 27, 30].

Infrared spectroscopy measurements on $PYR_{1(2O2)}$FSI were performed by means of a Bruker Vertex 70 V spectrometer at the SISSI beamline of ELETTRA Synchrotron, while measurements on $PYR_{1(2O1)}$TFSI were performed by means of a Bruker Vertex 125 HR spectrometer at the AILES beamline of Soleil Synchrotron [31, 32]. In both cases, we used an MCT detector and a KBr beamsplitter; the spectral resolution was fixed at 1 cm^{-1}. At ELETTRA, a thin layer of ionic liquid was placed between two CsI windows and mounted on a Heflow Helitran LT3 cryostat. At Soleil, a thin ionic liquid film was placed in a vacuum sealed cell (for liquids) with diamond windows and mounted on a CryoMac cryopump. In both cases, the samples were cooled down to ~130 K with a temperature rate of ~5 K min^{-1}, which allows reaching a glass state at low temperatures [26–28, 33].

2.2. Computational. Preliminary calculations of the conformers of PYR_{14}, $PYR_{1(2O1)}$, and $PYR_{1(2O1)}$ cations were performed using the Spartan software [34, 35] at the molecular mechanics level. They show 33, 27, and 40 possible conformers, respectively. All possible geometries were optimized by means of DFT calculations, using the B3LYP functional and the 6-31G** basis set. This particular choice of basis set and theory was extensively used in previous literature in order to calculate the infrared and Raman spectra of ions composing ILs [2–4, 8, 36]. We calculated the infrared vibration frequencies and intensities for all the geometries having energy within 3.5 kJ mol^{-1} from that of the lowest energy conformer of each ion. The visualization of the ions was performed by means of the wxMacMolPlt software [37]. For each cation, the IR spectrum was simulated by summing Gaussian curves centered at each calculated IR vibration frequency with a fixed 10 cm^{-1} peak width. As reported in Section 3, the good coincidence of the calculated vibration lines with the experimental absorption of the two ILs is itself a proof of the validity of the model based on the combination of theory and basis set presently used, which allows an easy study of the conformers of the cations. However, one must remember that, using the approach based on the calculations on single ions, one cannot obtain information about the interaction between anions and cations.

3. Results and Discussion

3.1. DFT Calculations of the Conformers of the Cations. In Figure 1, we report the structure of the lowest energy conformers of PYR_{14}. As already reported in [14, 16], the equatorial-envelope conformer has the lowest energy. The axial-envelope and the twist configurations possess slightly higher energies: 1.8 and 3.0 kJ mol, respectively. In all cases, the side chain is in all-*trans* configuration; geometries with different configurations of the alkyl chain have higher energies.

Figures 2 and 3 display the geometries of the lowest energy conformers of the $PYR_{1(2O1)}$ and $PYR_{1(2O2)}$ cations, respectively, calculated at the B3LYP/6-31G** level, together with their relative energy differences. For both ions, the lowest energy conformer has equatorial-envelope geometry. However, differently from the case of PYR_{14}, the side chain is not in an all-*trans* configuration: for $PYR_{1(2O1)}$ it presents a *cis-trans* structure (Conf. 1 in Figure 2) while, for $PYR_{1(2O2)}$, it displays a *cis-trans-trans* geometry (Conf. 1 and Conf. 2

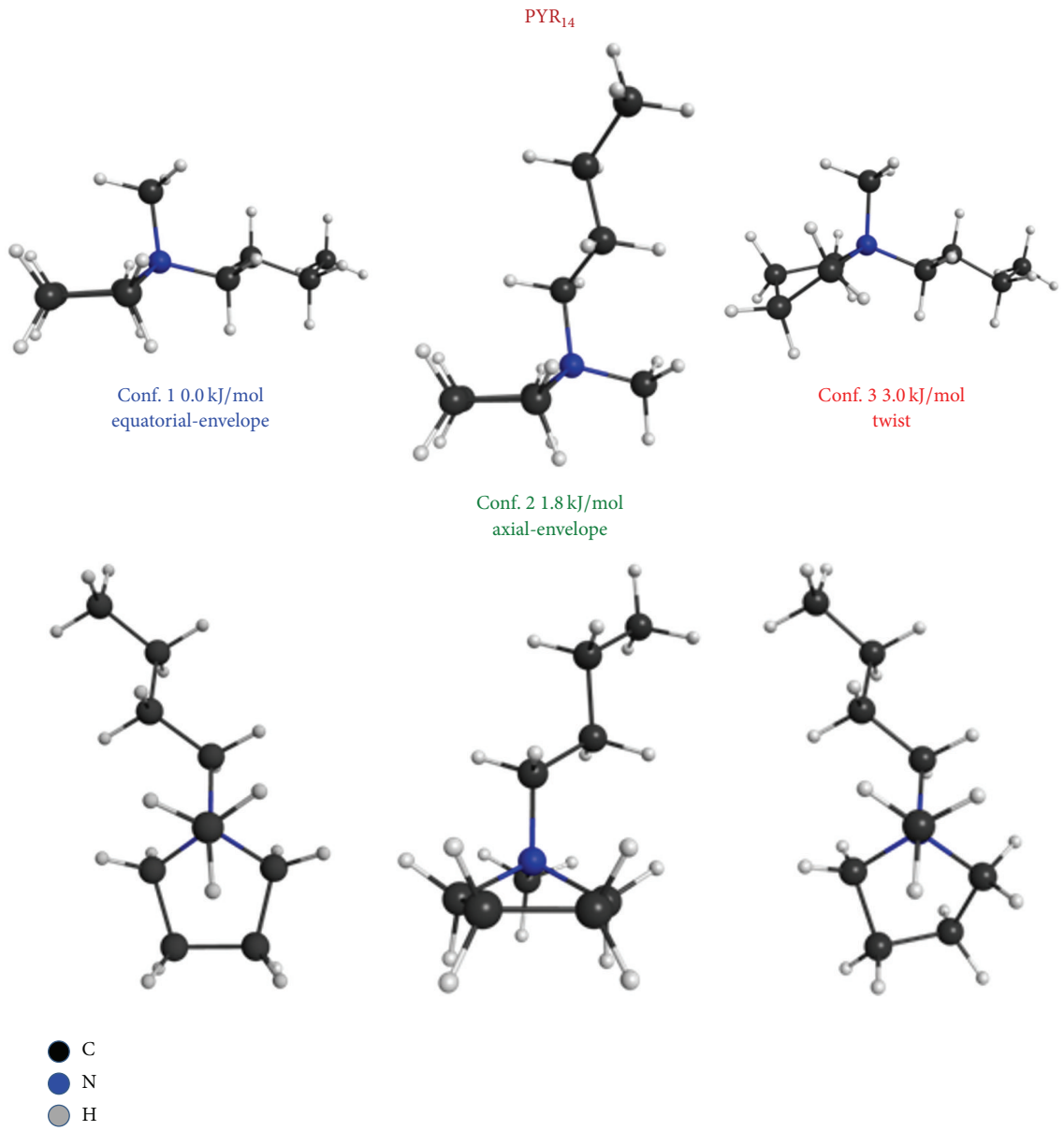

Figure 1: Optimized geometry of the lowest energy conformers of PYR_{14} projected on two different planes.

in Figure 3). For both cations, the conformers with the next higher energy are those with the twist structure of the pyrrolidinium ring (Conf. 2 in Figure 2 and Conf. 3 in Figure 3) and, subsequently, with the envelope pyrrolidinium geometry and the side chain at the axial position with respect to the ring (Conf. 3 and Conf. 4 in Figure 2 and Conf. 4 in Figure 3). For higher energies, the pyrrolidinium is in the envelope configuration, while the chain starts to be folded (see Figures 2 and 3). Among the conformers of $PYR_{1(2O1)}$ and $PYR_{1(2O2)}$ one can also find those with the side chain in the all-*trans* configuration; however, those conformers have higher energy than that of the lowest conformer by at least 20 kJ mol^{-1}, so that at ambient temperature they have a negligible population.

The calculated vibration frequency and IR intensity values of the lowest energy conformers of $PYR_{1(2O1)}$ and $PYR_{1(2O2)}$ are reported in Tables 1 and 2, for the frequency range of 800–1100 cm^{-1}, while the calculated absorbance is reported in Figures 4 and 5. The choice of this particular spectral range was motivated by the absence of absorption lines due to TFSI (from ~790 to ~1060 cm^{-1}) [7] or due to FSI (from ~830 to ~1100 cm^{-1}) [38].

As conformers 3 and 4 of $PYR_{1(2O1)}$ and conformers 1 and 2 of $PYR_{1(2O2)}$ differ only on the orientation of the side chain, their IR spectra are identical and, therefore, in the following, we will report only the spectrum of one rotamer for each couple.

3.2. Comparison with Infrared Spectroscopy Measurements. In order to validate the previously reported computational approach, we compared the calculated absorption of the two pyrrolidinium cations with the absorbance of $PYR_{1(2O1)}$TFSI and $PYR_{1(2O2)}$FSI. To avoid contributions from the TFSI or

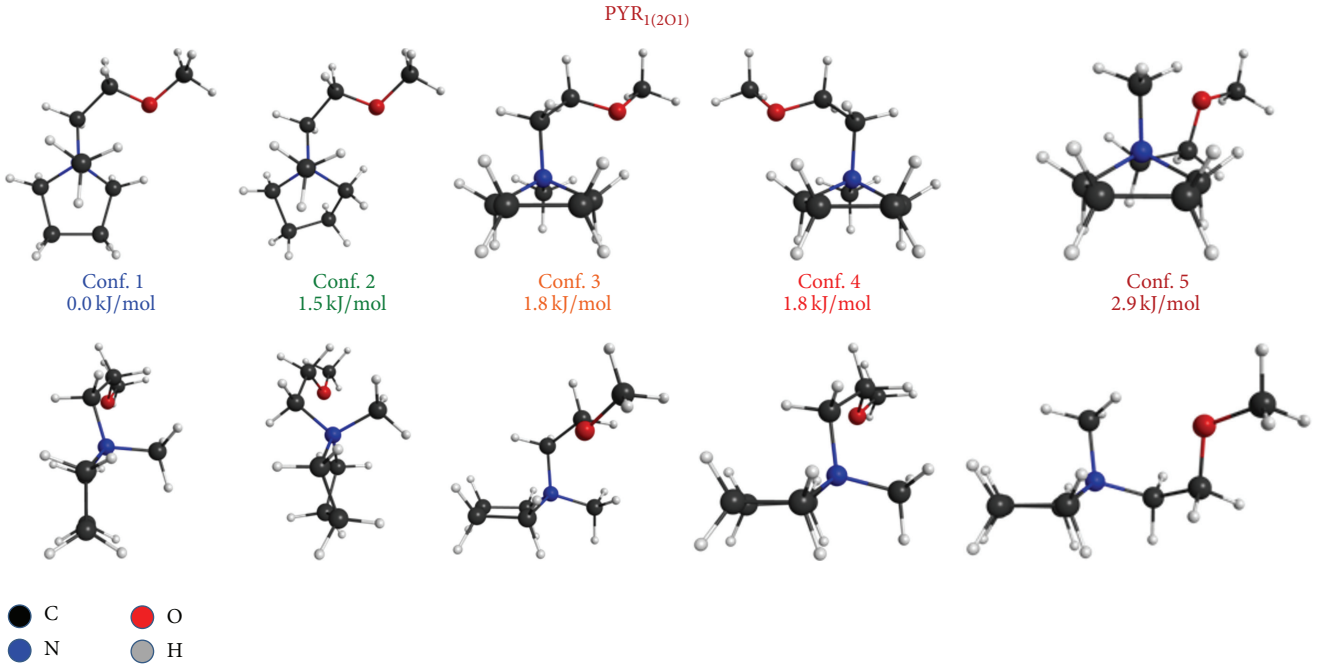

Figure 2: Optimized geometry of the lowest energy conformers of $PYR_{1(2O1)}$ projected on two different planes.

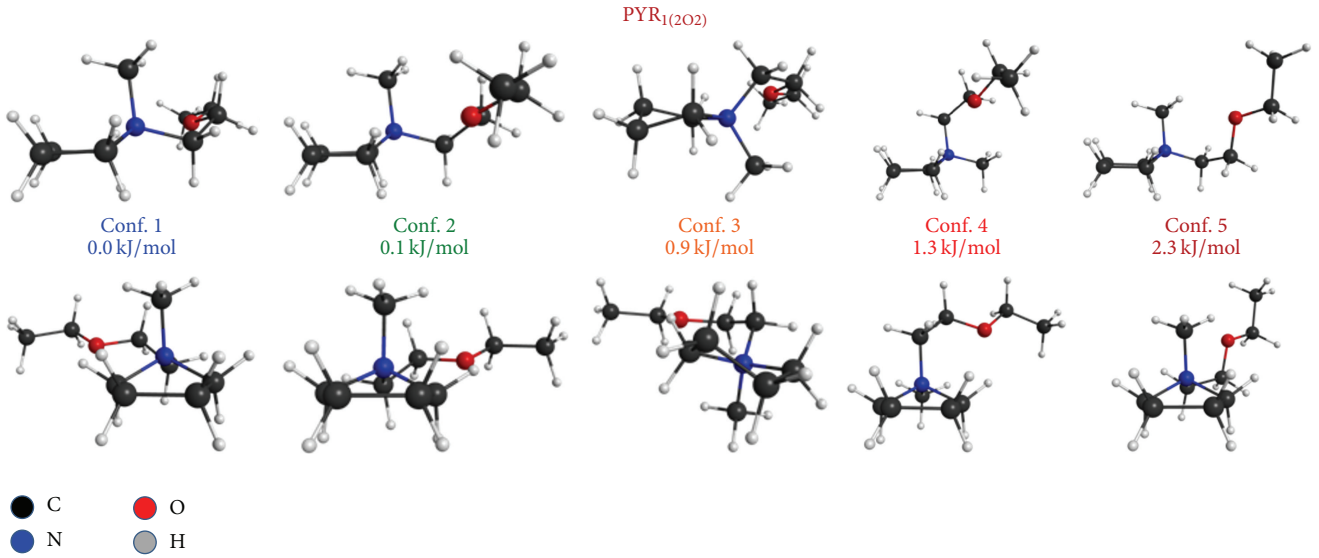

Figure 3: Optimized geometry of the lowest energy conformers of $PYR_{1(2O2)}$ projected on two different planes.

FSI anions, we limited our comparison to the spectral range between 800 and 1060 cm^{-1} for $PYR_{1(2O1)}$TFSI and from 860 to 1100 cm^{-1} for $PYR_{1(2O2)}$FSI. Indeed, in this spectral range, no contributions from the anions were previously reported [7, 38].

The absorbance spectra measured at two temperatures (e.g., around room temperature and at 130–140 K) for the two selected ionic liquids are reported in Figures 4 and 5. Both $PYR_{1(2O1)}$TFSI and $PYR_{1(2O2)}$FSI display several absorption bands in the considered spectral range. They are broader around room temperature, while they become sharper at low temperature. In many cases, at low temperatures, it is evident that the spectral lines are structured and composed of more than one contribution. Tables 3 and 4 report the frequencies of the absorption peaks found in the two compounds at both temperatures.

In Figure 4, one can observe that the peaks found in the experimental spectrum of $PYR_{1(2O1)}$TFSI nicely agree with those calculated for the lowest energy conformer, except for the peak located around 880 cm^{-1}, which is completely absent in Conf. 1 of $PYR_{1(2O1)}$. However, sharp features around 870 cm^{-1} are present in the calculated spectra of Conf. 2,

Table 1: Calculated frequency and intensity of the vibrations of the lowest energy conformers of $PYR_{1(2O1)}$ in the frequency range between 800 and 1100 cm^{-1} at the B3LYP/6-31G** level.

Conf. 1		Conf. 2		Conf. 3 = Conf. 4		Conf. 5	
Frequency (cm^{-1})	Intensity (km/mol)	Frequency (cm^{-1})	Intensity (km/mol)	Frequency (cm^{-1})	Intensity (km/mol)	Frequency (cm^{-1})	Intensity (km/mol)
804	5.02	843	5.05	806	2.31	823	8.75
821	7.49	868	24.46	863	4.52	825	2.75
855	7.38	881	7.5	872	35.36	848	9.33
900	3.5	922	6.41	905	9.46	901	4.95
911	29.15	933	15.13	936	3.52	917	13.43
941	17.92	954	6.19	984	0.56	933	25.87
949	2.88	989	9.6	993	6.86	942	2.37
1002	7.42	997	9.63	1009	13.33	995	2.37
1009	4.65	1029	7.2	1037	23.57	1006	20.81
1037	8.2	1044	71.03	1044	57.1	1037	60.23

Table 2: Calculated frequency and intensity of the vibrations of the lowest energy conformers of $PYR_{1(2O2)}$ in the frequency range between 800 and 1100 cm^{-1} at the B3LYP/6-31G** level.

Conf. 1 = Conf. 2		Conf. 3		Conf. 4		Conf. 5	
Frequency (cm^{-1})	Intensity (km/mol)	Frequency (cm^{-1})	Intensity (km/mol)	Frequency (cm^{-1})	Intensity (km/mol)	Frequency (cm^{-1})	Intensity (km/mol)
816	5.79	831	1.02	801	9.78	821	3
828	0.7	844	5.34	809	0.41	823	6.21
843	7.32	857	15.39	830	0.64	826	1.47
899	1.06	876	14.48	847	6.58	842	13.76
912	33.05	921	5.92	873	35.95	902	1.21
919	2.6	930	6.55	905	9.45	914	15.36
943	14.33	940	12.24	925	0.24	928	9.52
976	15.08	974	17.02	960	16.34	942	3.65
1003	12.59	990	12.89	986	0.77	961	28.96
1005	3.91	1000	10.18	1001	13.18	1001	15.96
1039	9.27	1029	9.7	1012	9.42	1011	8.64
1059	65.05	1053	6.19	1041	9.47	1050	37.93
1064	2.28	1061	60.61	1058	64.79	1063	26.61
				1070	4.98	1069	11.4

Table 3: Experimental vibration frequencies (in cm^{-1}) of $PYR_{1(2O1)}$TFSI measured at 280 K and 140 K.

280 K	140 K
844	822
879	845
904	882
935	901
996	910
	929
	939
1039	970
	990
	1000
	1039

Table 4: Experimental vibration frequencies (in cm^{-1}) of $PYR_{1(2O2)}$FSI measured at 300 K and 130 K.

300 K	130 K
875	860
903	881
936	900
960	908
990	939
998	946
1033	964
	994
1053	1002
	1039
	1056

Conf. 3, and Conf. 4 (the last one is not shown as it is identical to Conf. 3). Therefore, we suggest the presence of at least these four conformers of the pyrrolidinium cation. Indeed, the low energy difference among them supports the occurrence of dynamic equilibrium of those rotamers. In this framework, one can easily explain the asymmetry of the experimental absorption band located around 1000 cm^{-1}, which is evident at room temperature, and its splitting at low temperatures.

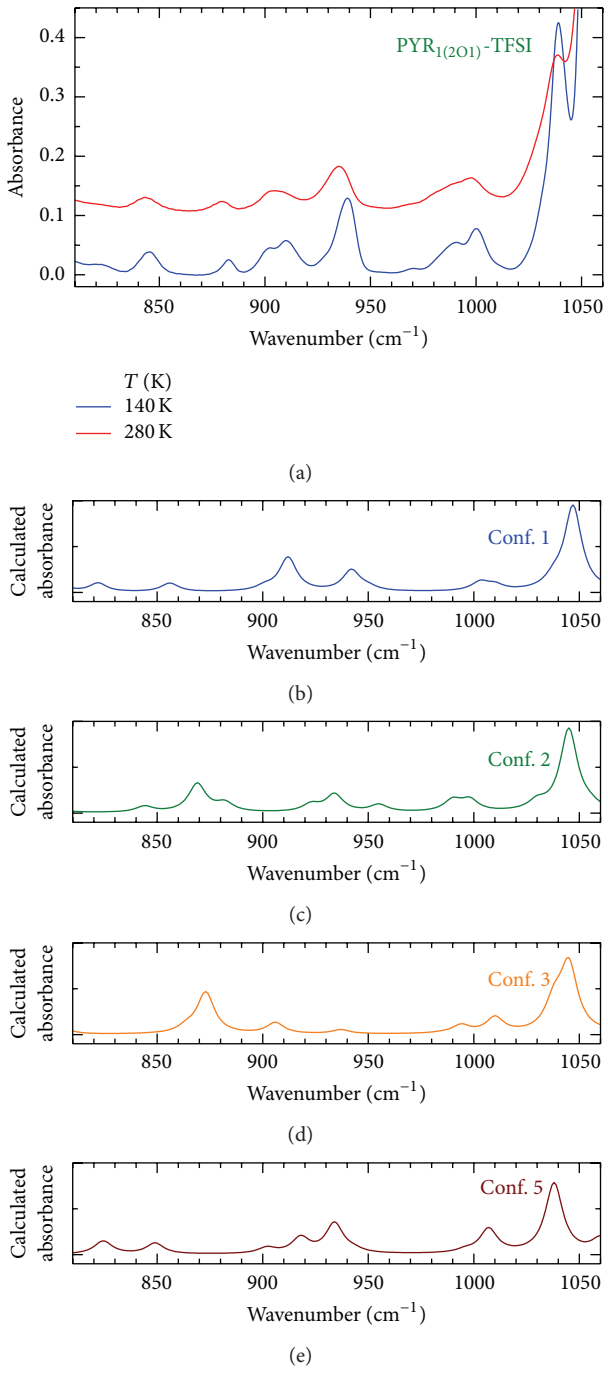

FIGURE 4: Comparison of the absorbance of $PYR_{1(2O1)}$TFSI measured at 280 and 140 K (a) and the calculated absorbance spectra of four conformers of $PYR_{1(2O1)}$ (b–e).

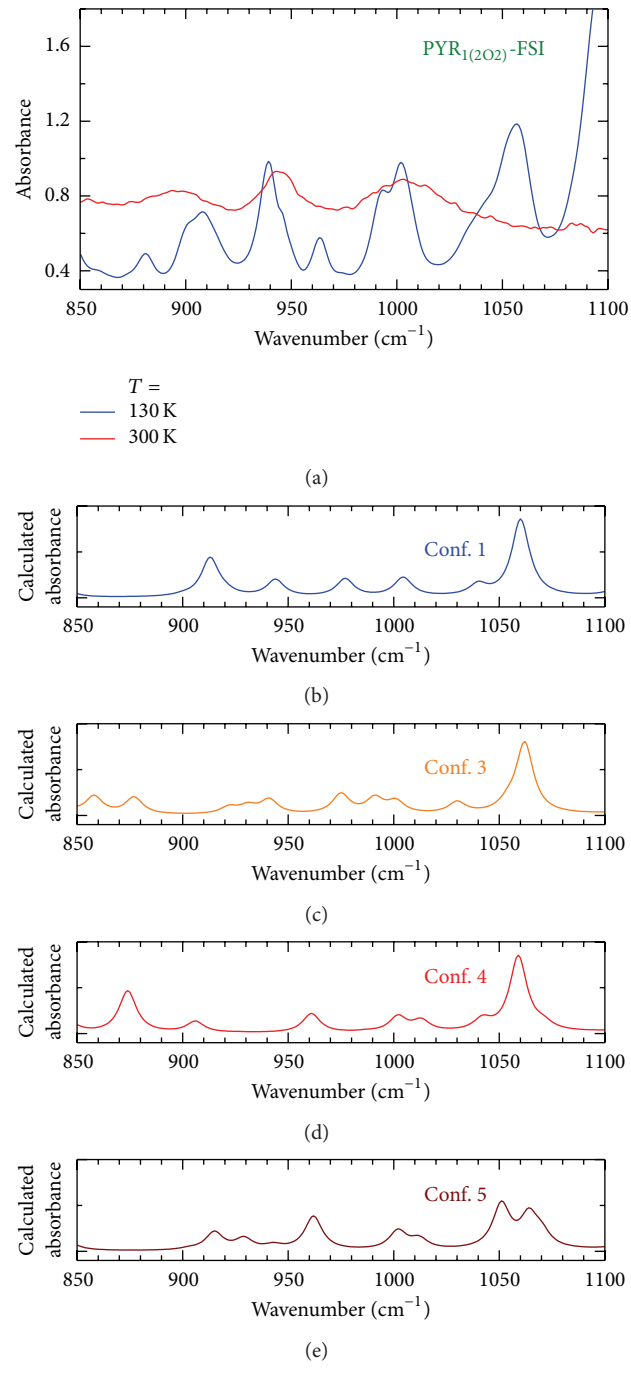

FIGURE 5: Comparison of the absorbance of $PYR_{1(2O2)}$FSI measured at 300 and 130 K (a) and the calculated absorbance spectra of four conformers of $PYR_{1(2O2)}$ (b–e).

Also in the case of $PYR_{1(2O2)}$FSI, there is a general good agreement between the experimental spectrum and the calculated absorbance of the lowest energy conformer. However, the presence of the experimental vibration line centered around 880 cm^{-1} suggests the occurrence of Conf. 3 and Conf. 4, which display absorption bands around this value. Such features are maintained also at 130 K.

The comparison of the experimental absorbance with the calculated vibrations lines evidences for both ILs that they exhibit more than one conformer of the pyrrolidinium cation at both measured temperatures. One can note that at low temperatures both ILs enter into a glass state. Therefore, the present measures indicate that both in the liquid and in the glassy state more than one conformer of pyrrolidinium is present.

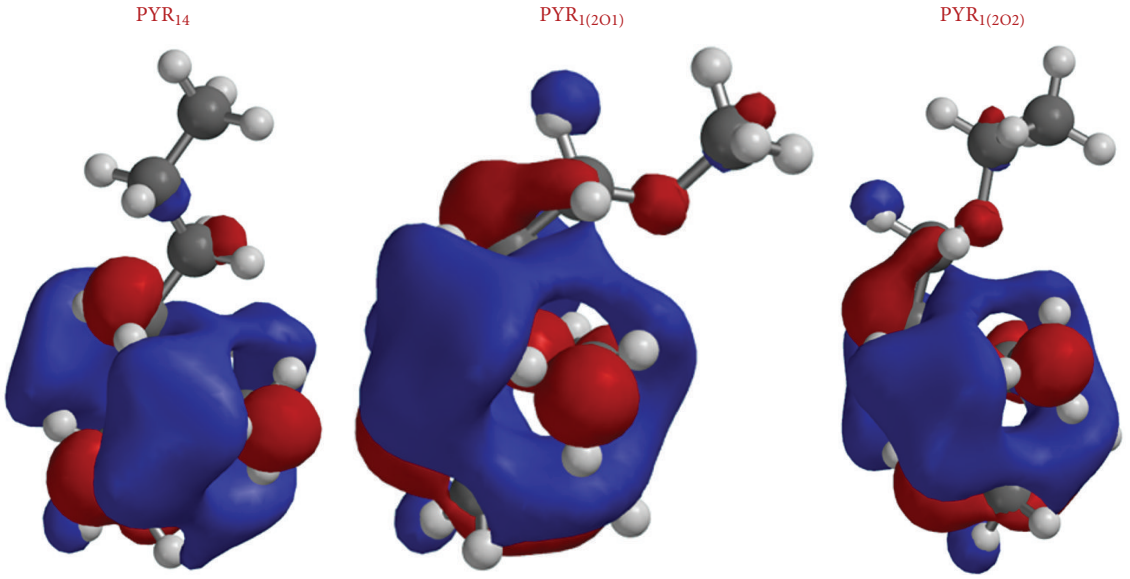

Figure 6: LUMO orbital of PYR_{14}, $PYR_{1(2O1)}$, and $PYR_{1(2O2)}$ calculated at the B3LYP/6-31G** level.

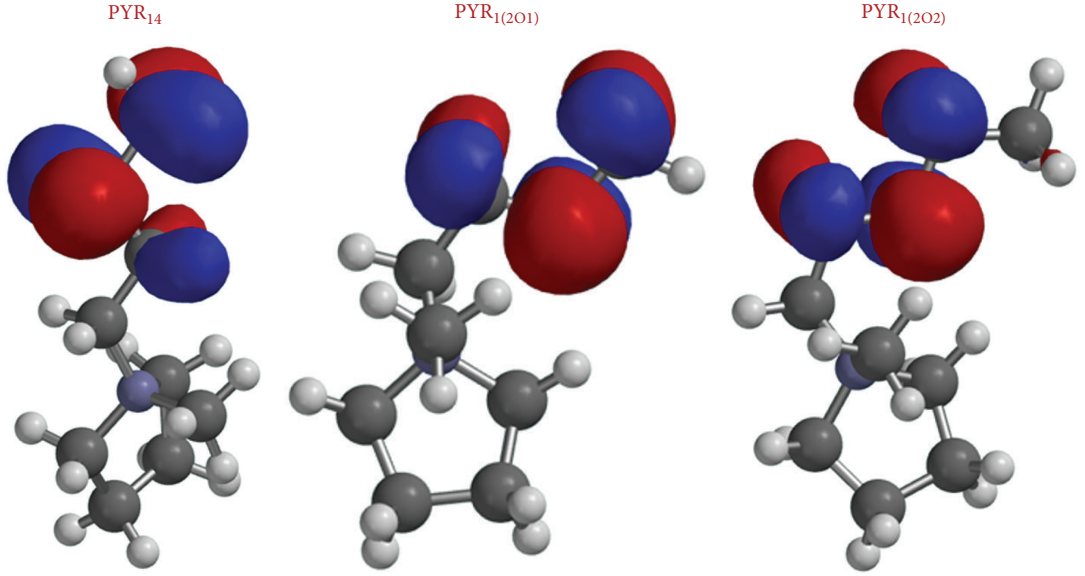

Figure 7: HOMO orbital of PYR_{14}, $PYR_{1(2O1)}$, and $PYR_{1(2O2)}$ calculated at the B3LYP/6-31G** level.

For both ions, the presence of conformers of higher energy, starting from Conf. 5, cannot be excluded; indeed according to the Boltzmann distribution function their occurrence is possible. However, their low concentration and the superposition of most of their absorption lines with those of the lower energy conformers prevent easy detection.

It must be noted that the good coincidence of the calculated vibration lines with the experimental absorptions of the two ILs is a proof of the validity of the DFT calculations based on the B3LYP functional and the 6-31G** basis set for the studied ions.

3.3. Calculations of the HOMO and LUMO Orbital. Once the structures of the lowest energy conformers have been confirmed by infrared spectroscopy measurements, the investigation is extended to the electronic properties. In Figure 6, the comparison among the calculated LUMO orbital of PYR_{14}, $PYR_{1(2O1)}$, and $PYR_{1(2O2)}$ calculated at the B3LYP/6-31G** level is reported. One can note that in all ions the LUMO extends on the whole pyrrolidinium ring and on the methyl group directly attached to it. For PYR_{14}, the orbital extends slightly also on three of the CH groups of the side alkyl chain. In the case of $PYR_{1(2O1)}$ and $PYR_{1(2O2)}$, the LUMO extends also on the fourth group of the side chain and displays bonding orbital between the first group and the second group of the chain, in contrast to PYR_{14}.

Also, the HOMO orbital of the three ions, reported in Figure 7, displays some differences. In all three ions, it extends

on the second, third, and fourth groups of the side chain. However, while in PYR_{14} the orbital on the second group is smaller than that of the third and fourth atoms of the chain, in $PYR_{1(2O1)}$ and $PYR_{1(2O2)}$ this difference is much smaller.

4. Conclusions

To summarize, an investigation of the conformers of two pyrrolidinium cations containing an ethoxy group in the main alkyl side chain has been performed by means of DFT calculations and validated by means of infrared absorbance measurements as a function of temperature. The lowest energy conformer of both pyrrolidinium cations has equatorial-envelope geometry. However, the side chain does not have all-*trans* geometry, as in the case of the prototype PYR_{14}, but has a *cis-trans* configuration for $PYR_{1(2O1)}$ and a *cis-trans-trans* structure for $PYR_{1(2O2)}$. For both ions, the conformers with the next higher energies are those with the twist structure of the pyrrolidinium ring and subsequently with the envelope geometry of pyrrolidinium and the side chain at the axial position with respect to the ring. Moreover, calculations indicate that the LUMO orbital extends more along the alkyl side chain in $PYR_{1(2O1)}$ and $PYR_{1(2O2)}$ than in the parent ion 1-butyl-1-methylpyrrolidinium (PYR_{14}).

Competing Interests

The authors declare that they have no competing interests.

Acknowledgments

The authors wish to thank P. Roy and J.-B. Brubach for assistance at the AILES beamline of Synchrotron Soleil during beamtime no. 20150313 and A. Perucchi and P. Di Pietro for assistance at the SISSI beamline of ELETTRA Synchrotron. This study was partially financed by ELETTRA Synchrotron for beamtime no. 20145151.

References

[1] M. A. Navarra, "Ionic liquids as safe electrolyte components for Li-metal and Li-ion batteries," *Material Research Society Bulletin*, vol. 38, no. 7, pp. 548–553, 2013.

[2] F. M. Vitucci, D. Manzo, M. A. Navarra et al., "Low-temperature phase transitions of 1-butyl-1-methylpyrrolidinium bis(trifluoromethanesulfonyl)imide swelling a polyvinylidene-fluoride electrospun membrane," *The Journal of Physical Chemistry C*, vol. 118, no. 11, pp. 5749–5755, 2014.

[3] K. Fujii, T. Fujimori, T. Takamuku, R. Kanzaki, Y. Umebayashi, and S.-I. Ishiguro, "Conformational equilibrium of bis(trifluoromethanesulfonyl) imide anion of a room-temperature ionic liquid: Raman spectroscopic study and DFT calculations," *Journal of Physical Chemistry B*, vol. 110, no. 16, pp. 8179–8183, 2006.

[4] J. N. Canongia Lopes, K. Shimizu, A. A. H. Pádua et al., "A tale of two ions: the conformational landscapes of bis(trifluoromethanesulfonyl)amide and *N,N*-dialkylpyrrolidinium," *The Journal of Physical Chemistry B*, vol. 112, no. 5, pp. 1465–1472, 2008.

[5] F. M. Vitucci, O. Palumbo, F. Trequattrini et al., "Interaction of 1-butyl-1-methylpyrrolidinium bis(trifluoromethanesulfonyl)imide with an electrospun PVdF membrane: Temperature dependence of the concentration of the anion conformers," *Journal of Chemical Physics*, vol. 143, no. 9, Article ID 094707, 2015.

[6] F. Capitani, F. Trequattrini, O. Palumbo, A. Paolone, and P. Postorino, "Phase transitions of PYR_{14}-TFSI as a function of pressure and temperature: the competition between smaller volume and lower energy conformer," *Journal of Physical Chemistry B*, vol. 120, pp. 2921–2928, 2016.

[7] F. M. Vitucci, F. Trequattrini, O. Palumbo, J.-B. Brubach, P. Roy, and A. Paolone, "Infrared spectra of bis(trifluoromethanesulfonyl)imide based ionic liquids: experiments and DFT simulations," *Vibrational Spectroscopy*, vol. 74, pp. 81–87, 2014.

[8] M. Herstedt, M. Smirnov, P. Johansson et al., "Spectroscopic characterization of the conformational states of the bis(trifluoromethanesulfonyl)imide anion ($TFSI^-$)," *Journal of Raman Spectroscopy*, vol. 36, no. 8, pp. 762–770, 2005.

[9] S. N. Suarez, A. Rúa, D. Cuffari et al., "Do TFSA anions slither? Pressure exposes the role of TFSA conformational exchange in self-diffusion," *The Journal of Physical Chemistry B*, vol. 119, no. 46, pp. 14756–14765, 2015.

[10] M. Shukla, H. Noothalapati, S. Shigeto, and S. Saha, "Importance of weak interactions and conformational equilibrium in N-butyl-N-methylpiperidinium bis(trifluromethanesulfonyl) imide room temperature ionic liquids: vibrational and theoretical studies," *Vibrational Spectroscopy*, vol. 75, pp. 107–117, 2014.

[11] J.-C. Lassègues, J. Grondin, C. Aupetit, and P. Johansson, "Spectroscopic identification of the lithium ion transporting species in LiTFSI-doped ionic liquids," *The Journal of Physical Chemistry A*, vol. 113, no. 1, pp. 305–314, 2009.

[12] A. Martinelli, A. Matic, P. Jacobsson, L. Börjesson, A. Fernicola, and B. Scrosati, "Phase behavior and ionic conductivity in lithium bis(trifluoromethanesulfonyl)imide-doped ionic liquids of the pyrrolidinium cation and bis(trifluoromethanesulfonyl)imide anion," *Journal of Physical Chemistry B*, vol. 113, no. 32, pp. 11247–11251, 2009.

[13] A. Martinelli, A. Matic, P. Johansson et al., "Conformational evolution of TFSI- in protic and aprotic ionic liquids," *Journal of Raman Spectroscopy*, vol. 42, no. 3, pp. 522–528, 2011.

[14] T. Fujimori, K. Fujii, R. Kanzaki et al., "Conformational structure of room temperature ionic liquid *N*-butyl-*N*-methylpyrrolidinium bis(trifluoromethanesulfonyl) imide—Raman spectroscopic study and DFT calculations," *Journal of Molecular Liquids*, vol. 131-132, pp. 216–224, 2007.

[15] H. Ishida, "Conformations of pyrrolidinium ion studied by molecular orbital calculations," *Zeitschrift für Naturforschung*, vol. 55, no. 6-7, pp. 665–666, 2000.

[16] O. Palumbo, F. Trequattrini, F. M. Vitucci, and A. Paolone, "Relaxation dynamics and phase transitions in ionic liquids: viscoelastic properties from the liquid to the solid state," *The Journal of Physical Chemistry B*, vol. 119, no. 40, pp. 12905–12911, 2015.

[17] K. Fujil, S. Seki, S. Fukuda et al., "Anion conformation of low-viscosity room-temperature ionic liquid 1-ethyl-3-methylimidazolium bis(fluorosulfonyl) imide," *The Journal of Physical Chemistry B*, vol. 111, no. 44, pp. 12829–12833, 2007.

[18] Y. Shimizu, K. Fujii, M. Imanari, and K. Nishikawa, "Phase behavior of a piperidinium-based room-temperature ionic

liquid exhibiting scanning rate dependence," *Journal of Physical Chemistry B*, vol. 119, no. 38, pp. 12552–12560, 2015.

[19] M. C. C. Ribeiro, "High viscosity of imidazolium ionic liquids with the hydrogen sulfate anion: a Raman spectroscopy study," *The Journal of Physical Chemistry B*, vol. 116, no. 24, pp. 7281–7290, 2012.

[20] Y. Jeon, J. Sung, C. Seo et al., "Structures of ionic liquids with different anions studied by infrared vibration spectroscopy," *The Journal of Physical Chemistry B*, vol. 112, no. 15, pp. 4735–4740, 2008.

[21] J. Grondin, J.-C. Lassègues, D. Cavagnat, T. Buffeteau, P. Johansson, and R. Holomb, "Revisited vibrational assignments of imidazolium-based ionic liquids," *Journal of Raman Spectroscopy*, vol. 42, no. 4, pp. 733–743, 2011.

[22] X. Zhu, C. Yuan, H. Li et al., "Successive disorder to disorder phase transitions in ionic liquid [HMIM][BF4] under high pressure," *Journal of Molecular Structure*, vol. 1106, pp. 70–75, 2016.

[23] T. A. Lima, V. H. Paschoal, L. F. Faria et al., "Comparing two tetraalkylammonium ionic liquids. II. Phase transitions," *The Journal of Chemical Physics*, vol. 144, no. 22, p. 224505, 2016.

[24] F. Capitani, C. Fasolato, S. Mangialardo, S. Signorelli, L. Gontrani, and P. Postorino, "Heterogeneity of propylammonium nitrate solid phases obtained under high pressure," *Journal of Physics and Chemistry of Solids*, vol. 84, no. 1, pp. 13–16, 2015.

[25] Y. L. Verma and R. K. Singh, "Conformational states of ionic liquid 1-ethyl-3-methylimidazolium bis(trifluoromethylsulfonyl)imide in bulk and confined silica nanopores probed by crystallization kinetics study," *The Journal of Physical Chemistry C*, vol. 119, no. 43, pp. 24381–24392, 2015.

[26] G. B. Appetecchi, S. Scaccia, C. Tizzani, F. Alessandrini, and S. Passerini, "Synthesis of hydrophobic ionic liquids for electrochemical applications," *Journal of the Electrochemical Society*, vol. 153, no. 9, pp. A1685–A1691, 2006.

[27] G. B. Appetecchi, M. Carewska, M. Montanino, F. Alessandrini, and S. Passerini, "LiFSI-PYR_{1A}FSI binary electrolyte mixtures for lithium batteries," *ECS Transactions*, vol. 25, no. 36, pp. 49–60, 2010.

[28] J. Reiter, E. Paillard, L. Grande, M. Winter, and S. Passerini, "Physicochemical properties of *N*-methoxyethyl-*N*-methylpyrrolidinum ionic liquids with perfluorinated anions," *Electrochimica Acta*, vol. 91, pp. 101–107, 2013.

[29] S. Ferrari, E. Quartarone, P. Mustarelli et al., "A binary ionic liquid system composed of *N*-methoxyethyl-*N*-methylpyrrolidinium bis(trifluoromethanesulfonyl)-imide and lithium bis(trifluoromethanesulfonyl)imide: a new promising electrolyte for lithium batteries," *Journal of Power Sources*, vol. 194, no. 1, pp. 45–50, 2009.

[30] G. B. Appetecchi, M. Montanino, M. Carewska, M. Moreno, F. Alessandrini, and S. Passerini, "Chemical-physical properties of bis(perfluoroalkylsulfonyl)imide-based ionic liquids," *Electrochimica Acta*, vol. 56, no. 3, pp. 1300–1307, 2011.

[31] P. Roy, M. Guidi Cestelli, A. Nucara et al., "Spectral distribution of infrared synchrotron radiation by an insertion device and its edges: a comparison between experimental and simulated spectra," *Physical Review Letters*, vol. 84, no. 3, pp. 483–486, 2000.

[32] P. Roy, J.-B. Brubach, P. Calvani et al., "Infrared synchrotron radiation: from the production to the spectroscopic and microscopic applications," *Nuclear Instruments and Methods in Physics Research A*, vol. 467-468, pp. 426–436, 2001.

[33] Q. Zhou, W. A. Henderson, G. B. Appetecchi, M. Montanino, and S. Passerini, "Physical and electrochemical properties of *N*-alkyl-*N*-methylpyrrolidinium bis(fluorosulfonyl)imide ionic liquids: PY_{13}FSI and PY_{14}FSI," *The Journal of Physical Chemistry B*, vol. 112, no. 43, pp. 13577–13580, 2008.

[34] Y. Shao, L. F. Molnar, Y. Jung et al., "Advances in methods and algorithms in a modern quantum chemistry program package," *Physical Chemistry Chemical Physics*, vol. 8, no. 27, pp. 3172–3191, 2006.

[35] W. J. Hehre, *Guide to Molecular Mechanics and Quantum Chemical Calculations*, Wavefunction, Irvine, Calif, USA, 2003.

[36] F. M. Vitucci, F. Trequattrini, O. Palumbo et al., "Stabilization of different conformers of bis(trifluoromethanesulfonyl)imide anion in ammonium-based ionic liquids at low temperatures," *The Journal of Physical Chemistry A*, vol. 118, no. 38, pp. 8758–8764, 2014.

[37] B. M. Bode and M. S. Gordon, "MacMolPlt: a graphical user interface for GAMESS," *Journal of Molecular Graphics and Modelling*, vol. 16, no. 3, pp. 133–138, 1998.

[38] S. Gatto, O. Palumbo, S. Caramazza et al., "The infrared spectrum of bis(fluorosulfonyl)imide revisited: attractive performances of the PBE0/6-31G** model," *Vibrational Spectroscopy*, vol. 82, pp. 16–21, 2016.